

© 2017 IEEE. Personal use of this material is permitted. Permission from IEEE must be obtained for all other uses, in any current or future media, including reprinting/republishing this material for advertising or promotional purposes, creating new collective works, for resale or redistribution to servers or lists, or reuse of any copyrighted component of this work in other works.

Digital Object Identifier (DOI): 10.1109/MPEL.2017.2692381

IEEE Power Electronics Magazine (Volume:4, Issue:2) June 2017

The Smart Transformer: a Solid-State-Transformer tailored to provide ancillary services to the distribution grid

Levy Ferreira Costa
Giovanni De Carne
Giampaolo Buticchi
Marco Liserre

Suggested Citation

L. Ferreira Costa, G. De Carne, G. Buticchi and M. Liserre, "The Smart Transformer: A solid-state transformer tailored to provide ancillary services to the distribution grid," in *IEEE Power Electronics Magazine*, vol. 4, no. 2, pp. 56-67, June 2017.

The Smart Transformer: a Solid-State-Transformer tailored to provide ancillary services to the distribution grid

Levy Costa, Giovanni De Carne, Giampaolo Buticchi Marco Liserre

Abstract: The Solid State Transformer (SST) was conceived as a replacement of the conventional power transformer (CPT) with lower volume and weight. The Smart Transformer (ST) is a SST that provides ancillary services to the distribution and transmission grids in order to optimize their performance. Hence, the focus shifts from hardware advantages to functionalities. One of the most desired functionality is the DC connectivity to enable a hybrid distribution system. For this reason, the ST architecture shall be composed of at least two power stages. The standard design procedure for this kind of system is to design each power stage for the maximum load. However, this design approach might limit the additional services, like the reactive power compensation on the MV side and it does not take into account the load regulation capability of the Smart Transformer on the low voltage side. If the SST is tailored to the services that it shall provide, different stages have different design, so that the ST is not a mere application of the SST anymore, but an entirely new subject.

I. Introduction

The integration of renewable energy systems and new loads, like EVs, has changed the distribution grid. The grid, once passive and static with limited amount of distributed generators, is now active and dynamic. The LV grid hosts, together with the residential and commercial loads, small size generators, in the range of hundreds of Watt to few hundreds of kW. This generation capability consists of diesel generators, gas microturbines, photovoltaics and micro wind turbines. Among these resources, there are the controllable ones (diesel and gas generators) and the ones, called renewables, that provide energy when available from natural sources (e.g., wind, sun irradiation, tides).

The last category has two main features: high power injection variability and distributed presence in the distribution grid. These generation units vary their power output with short-term forecast possibilities and not at the same time due to the different geographical distribution. The major challenges for the grid are the voltage control, frequency stability, reverse power flow, and protection systems coordination [1,3].

The Smart Transformer, a Solid State Transformer with control and communication functionalities, can represent a solution for many of the mentioned problems. The ST features cover a wide range of services, like the reactive power support in MV grids, DC connectivity at both medium- and low-voltage level, and load control in LV side. The ST is designed following a three-stage solution, with the isolation stage in the DC/DC converter. This solution enables the galvanic isolation between the two grids, guaranteeing the appliances safety during abnormal conditions (e.g., faults or lightning strikes). The ST basic design does not differ substantially from the Solid State Transformer concept. However, differently from the SST, designed mainly for traction applications or as mere 1-to1 replacement of conventional transformers, the ST shall be tailored to provide the previously mentioned services.

This article present the grid-tailored design approach for smart transformers, taking in account the load requirements (e.g., unbalanced conditions) and the services that can be provided to the grid (e.g., reactive power support). The proposed design approach shows how the ST can be undersized thanks to the higher control capability on the low voltage side or how the saving obtained due to such control actions on the low voltage side can be used to provide more services on the MV side.

II. The Smart Transformer concept

Several ST architectures have been proposed and classified in the literature. An overview of the possible architectures presenting several configurations has been presented in [4-7]. Among the possible configurations, the three-stage one (composed by: MV stage / DC/DC stage / LV stage) enables dc-link connectivity and also guarantees input/output decoupling of voltages and currents, providing the system control more degrees of freedom and making it the preferred candidate for an ST. To handle the MV level involved on the power conversion, modular architectures bring several advantages, such as low dv/dt (low electromagnetic interference emission), the potential to use standard LV-rating devices, and modularity, which allows for the implementation of redundant strategies to increase fault tolerance and availability. For these reasons, modular architectures are preferable for ST applications.

Fig. 1 shows the grid scenario in which the ST should operate, i.e. MV to LV connection with the availability of the DC Links preferably in both sides.

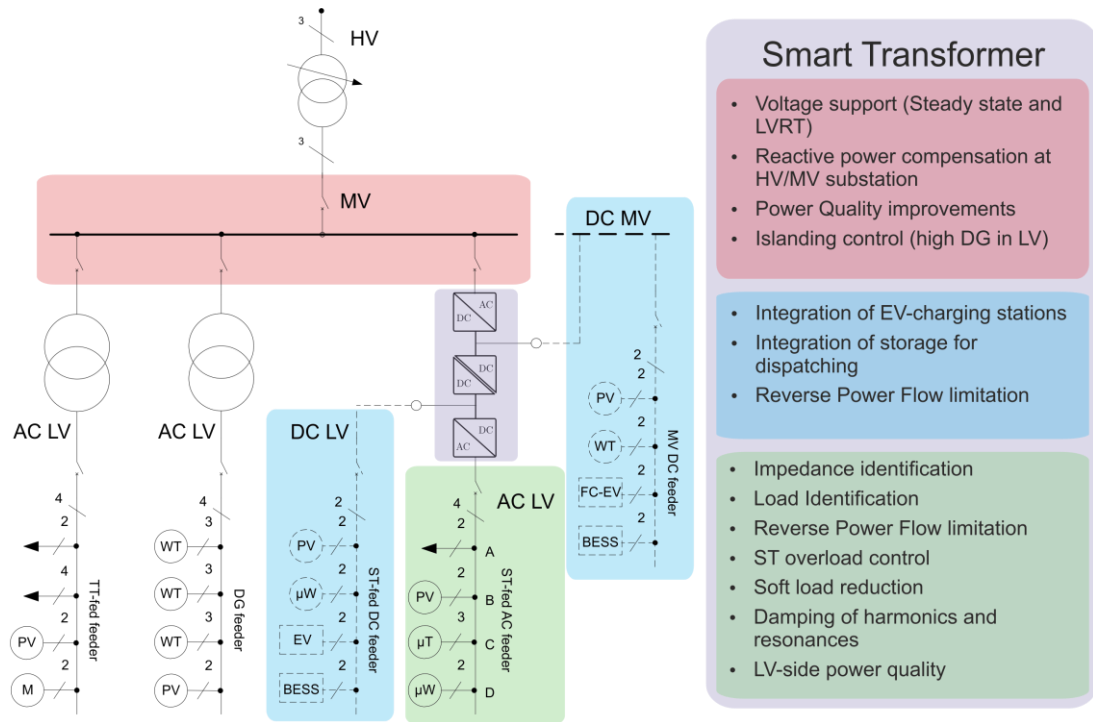


Fig. 1. The Smart Transformer (ST) and its role in the electric grid.

A. LV side

In the LV grid, the ST controls the voltage waveform. Independently from the load current request, the ST provides a sinusoidal voltage waveform with nominal amplitude and frequency. However, the ST can provide ancillary services modifying the voltage amplitude and frequency. It is well known that the loads power consumption depends on the voltage magnitude, as well as the grid-connected generators have frequency / power droop controllers to sustain the grid frequency during perturbations. The ST exploits these characteristic for modifying the load consumption / generator production in LV grid. The possible ancillary services provided by these features are the load identification and control [8], the soft load reduction [9], the reverse power flow limitation [10, 11] and the ST overload control [12]. In the first service, the sensitivities of active and reactive power to voltage and frequency variations are identified. These sensitivities are employed to increase the control accuracy: when the ST receives a power reduction request, the voltage controller reduces the voltage amplitude by the amount needed to achieve the desired power reduction. This service, called soft load reduction, allows participating to the transmission grid control, offering a power absorption control range of $\pm 10\%$. This is shown in Fig. 2, where the LV side control modifies the voltage in order to reduce the consumption at LV side. An additional 10% of control capability is given by the possibility to modify the frequency, interacting with the renewables.

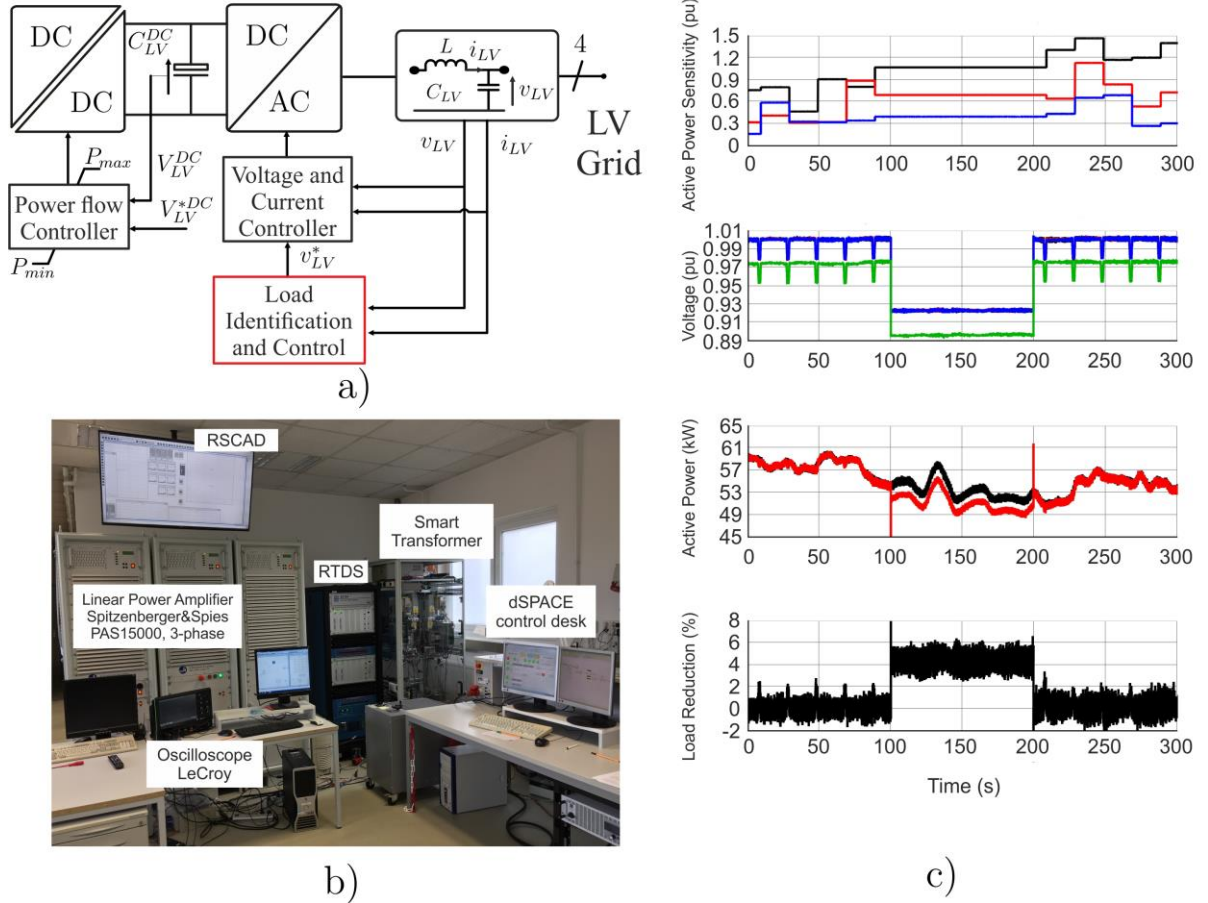


Fig. 2 Services to the LV grid. a) block scheme of the LV side control, b) experimental setup based on Real Time Digital Simulator, c) soft-load reduction experiment [8], from top to bottom: sensitivity coefficients, voltage profiles, power profile, percentage of shed load.

Taking into account these services, the most suitable topologies to implement the ST from the power electronics viewpoint are: voltage source inverter (VSI) four wires, based on the Full-Bridge (FB), T-type or Neutral-Point-Clamped (NPC) topologies [4]. Due to the requirement of the neutral conductor, the middle point dc-link is available, leading to an additional voltage balancing circuit. The two-level FB topology represents the simplest approach and a consolidated solution. On the other hand, the three-level topologies have been accepted as feasible solutions by industry; for this reason, the NPC or T-Type topologies would allow the use of 600-V devices, improving the output waveform and system efficiency at the same time.

B. DC/DC conversion

The availability of two DC stages allows for the creation of local or regional DC grids. The MV DC-link works as connection point between STs and can host new loads, like the fast charging-electric vehicles (FC-EV) stations and distributed resources, like large photovoltaic and wind power plants and battery energy storage systems (BESS). The LV DC-link offers instead the possibility to connect the DC loads directly to a LV DC grid, avoiding an intermediate conversion stage at the user's site. The DC links allow for the AC power flow separation between MV and LV grids. This feature enables controlling the two grids independently, with the only constrain of the active power link.

This power stage has strict requirements, such as high-rated power, high current capability on the LV side, and high-voltage capability, high frequency isolation, and high efficiency on the MV side. The basic configuration implies series-connected modules in the MV side and parallel-connected ones in the LV side.

The basic module of the DC/DC stage is based on an isolated DC/DC converter, implemented normally using the Dual Active Bridge (DAB) converter [13], or the Series Resonant Converter (SRC) [14]. An additional approach is the use of multiwinding-based topologies, such as the quadruple active bridge (QAB) [15] as a basic

cell. This converter presents the same advantages of the DAB converter, but with a lower number of high/medium frequency transformers. Following the configuration in [15], the converter has a lower number of auxiliary components (e.g. drivers, auxiliary power supply) in the LV side. Regardless the basic power module, the LV DC-link and/or MV DC-link are available for microgrids connection.

C. MV side

At the MV level, the ST controls the active current in order to keep the MV DC link voltage constant at the nominal value. The reactive power is controlled separately from the active power and represents a degree of freedom for the system control. The ST can inject reactive power for voltage support purpose, both in steady-state, controlling the voltage profile in the grid, and during transients, offering services like Low Voltage Ride Through (LVRT). With the help of communication, the ST can perform the power factor correction at the HV/MV substation, reducing the reactive power request to the transmission grid. The active power is the only link between the AC MV and LV smart transformer stages. Oscillating power components can be controlled separately from the active power. Thus, harmonic voltage and current compensation is possible.

The most promising topologies to implement the MV stage of the ST are the Cascaded H-Bridge (CHB) converter and Modular Multilevel Converter (MMC). Both converters share the same features: modularity, possibility of fault-tolerance implementation, multilevel operation, reduced dv/dt and filter size. On hand, the MMC presents the additional advantage to provide the DC link for connection of MVDC loads/sources. On the other hand, this topology requires a very complex control system, bulky filter in the dc side (when compared to the CHB topology) and high cost. For these reason, it has not been adopted for MV applications yet, but only in HV applications.

The CHB represents the most promising topology solution, thanks to its aforementioned advantages associated to a simple modulation and control system. Its main disadvantage, however, results to be the lack of a MVDC link for MVDC grids connectivity.

The NPC converter may be a possible topology to implement the MV stage and it represents a standard solution for MV applications. However, due to the voltage level of the MVDC link (normally more than 15 kV), series connection of IGBT is required. Furthermore, the NPC is not a modular solution and a bigger AC filter, compared to the previous converters, must be installed.

III. SST Topology selected for the Smart Transformer

To select the proper architecture of the modular three-stage ST, not only the power converter must be chosen, but also the number of modules plays an important role. In this section, these points are discussed and the ST architecture is selected, considering the grid specification presented in Table I. Regarding the MV side converter, the CHB topology is selected due to its simpler operation and control. In the LV side, a standard VSI is employed.

The DAB and the QAB converters are considered for the DC/DC stage because they offer power flow control. The ST architectures employing DAB and QAB as a building block of the DC/DC are shown in Fig. 3. In these figures, a unit is defined as a replaceable part of the ST and it is composed by the DC/DC converter associated to respective MV cell of the CHB connected to it, as can be seen in Fig. 3.

Table I. Grid specification

Grid Specification					
Rated Power	MVAC	LVAC	Grid frequency	Total MVDC link	LVDC link
1 MVA	10 kV	400 V	50 Hz	700 V	700 V

A. Number of Unit Selection

To select the number of modules, the constraints are: fault tolerance capability, IGBT blocking voltage, system complexity, number of components and rated power of the modules. All these parameters have influence on cost, reliability, efficiency and system complexity. The number of units is selected from the MV side viewpoint, taking the cost as the main parameter.

If a large number of modules is selected, the semiconductor blocking voltage of the MV side is reduced, but the total amount of parts (including auxiliary power supply, drivers, communication, etc.) and system complexity

increase considerably. Table II shows the main parameters of the ST MV side for different numbers of units, considering both DAB and QAB solutions. In this analysis, the available IGBT modules on the market from the main manufactures were considered and they are listed in Table VII of the Appendix A. For the cost analysis, IGBT modules from Powerex/Mitsubishi are assumed, as presented in Table VIII (Appendix A). As can be noticed in Table II, the MV side current is independent from the number of units, because the modules share the voltage and power among them in the MV side. Thus, the use of high voltage blocking IGBT's implies an underutilization of the devices, because they are normally available only for high current. Furthermore, the device cost is very high, leading to the most expensive solution, as presented in Table II. From the cost analysis, the most advantageous solution is employing 27 or 36 CHB cells (with a difference of only US\$ 720 between them). Considering also the implementation complexity and the number of components, 27 CHB cells represent to be most suitable solution and this design is considered for this work.

Table II. Main parameters of the MV side of the ST for different numbers of power units

N° of Units		Unit power level (kW)		N° of CHB cells	MV dc-link (kV)	IGBT voltage rating (kV)	Mean current (A)	IGBT current rating (A)	Cost (US\$)
QAB	DAB	QAB	DAB						
3	9	333.33	111.11	9	3.4	6.5	17.6	150	12402
6	18	166.67	55.56	18	1.7	3.3		75	19404
9	27	111.11	37.04	27	1.13	1.7		50	6480
12	36	83.33	27.78	36	0.85	1.2		50	5760
15	45	66.67	22.22	45	0.68	1.2		50	7200

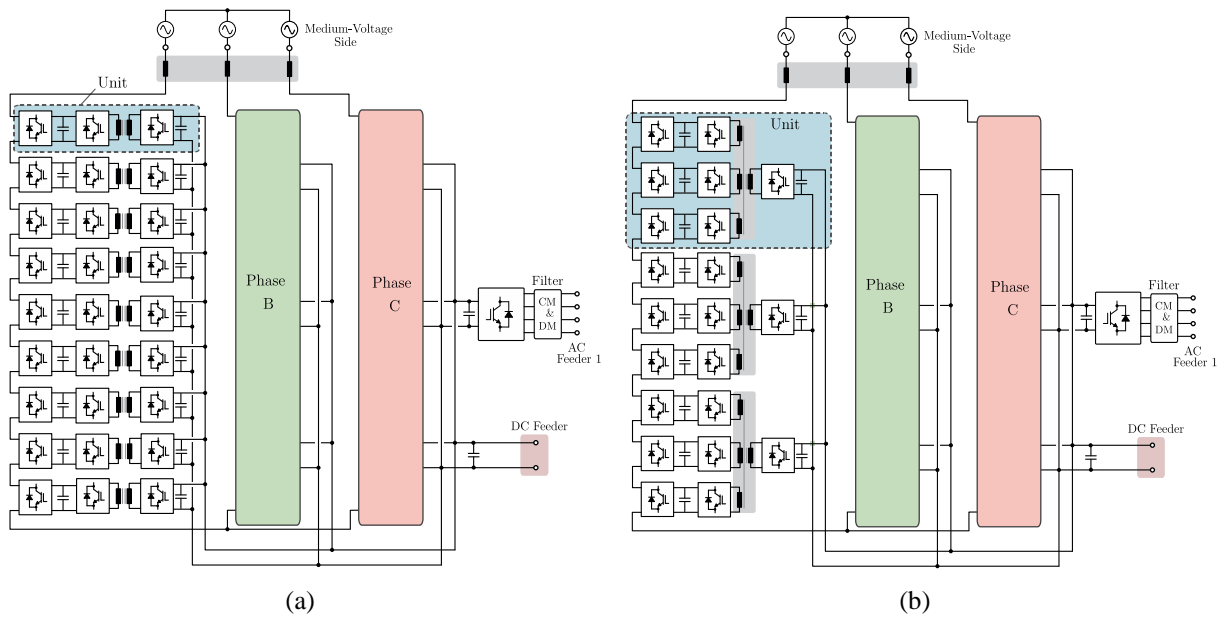


Fig. 3. Smart Transformer architecture considering two DC/DC solution: (a) DAB, (b) QAB.

B. QAB and DAB Converter Comparison

Since the DAB and QAB converters are the most promising topologies, they are compared in this work in terms of cost, efficiency, complexity and reliability. Both converters are designed assuming the specifications and parameters presented in Tables I and II. A phase-shift modulation is considered [15], with a nominal phase angle of 35° and switching frequency of $f_s = 20$ kHz. The detailed values obtained from the design are presented in Appendix B. A comparative analysis of both converters is presented in Table III, where the main parameters of the design are summarized and the components quantity and cost are presented.

The QAB converter has less LV cells, as well as fewer transformers. Consequently, the employed semiconductors and auxiliary components, such as gate-driver units (GDU), auxiliary power supplies (APS) and control and communication systems are also reduced, compared to the DAB solution. Although higher current rating devices are required to implement the LV cell of the QAB (see table III), the individual device cost does not differ much from the cost of the devices required by the DAB solution, as can be seen in Table VII. Consequently, the QAB converter presents as the most effective solution economically and practically,

since it uses fewer components. By using QAB instead DAB, a cost saving of US\$ 2350.08 (only in semiconductors) is achieved and this value can be higher if the auxiliary components are considered. Fig. 4 shows a qualitative comparison between the QAB and DAB converters. In balanced condition, both converters present the same performance from the efficiency viewpoint [15]. On the other hand, the control of the QAB presents higher complexity than the DAB one. Despite this fact, the QAB solution presents several advantages over the DAB solution, and then it is chosen to implement the DC/DC of the ST.

Table III. Comparative analysis of the DAB and QAB converters

Parameter	DAB		QAB
	LV side	MV side	LV side
Number of cells	27	27	9
IGBT current rating	50 A	50A	150A
IGBT voltage rating	1.2 kV	1.7 kV	1.2 kV
N° semiconductor	108	108	36
Total semiconductor cost	US\$ 4336,74	US\$ 6480	US\$ 1986,66
Auxiliary Power Supply	27	27	9
Gate Driver Unit	54	54	18
Control and comm system	27	27	9
N° of MFT	27		9
Isolation requirement	10 kV (prim-sec)		10 kV (prim-sec) 1.2 kV (sec-sec)
TOTAL COST	US\$ 10816,74		US\$ 8466,66

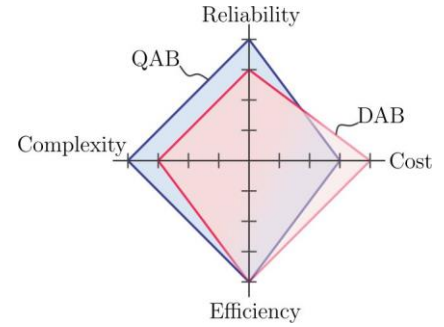


Fig. 4. Qualitative comparison of QAB and DAB performance characteristic.

IV. Proposed grid tailored approach

The ST design is a complex matter: the peak load consumption is difficult to be evaluated, and it is limited in the time to few hours for year. The actual procedure for sizing the conventional transformer is quite conservative, and it is based on the peak load. As highlighted in [16], this results in a transformer oversizing in the majority of the cases (63% in the study carried). Only few transformers have been adequately sized or undersized.

The classical SST design is based on equally sized converters and it comes from the conventional transformer sizing. As base case, the SST has been sized for 1 MVA power. The ST enables an improved load control, mainly in LV side. Modifying the voltage amplitude and frequency, the ST can interact with the LV generators and loads in order to modify the power consumption [9]. The possibility to reduce the active power consumption acting on the voltage is well known in North America, where the Conservation Voltage Reduction (CVR) is widely applied [17, 18]. The CVR exploits the transformer on-Line Tap Changers (LTC) to decrease the voltage in the downstream grid. Reducing the voltage, also the grid power consumption decreases. In [15] the energy saved along the year is estimated to be 4%, and the load peak reduction up to 4%. However, the CVR cannot evaluate on line the power reduction. The ST, implementing the On-Line Load Identification [8], is able to identify the load sensitivity to voltage and frequency variation, and thus to apply a more accurate control action, as shown in [9]. From the surveys' result in [19], the distribution system operators identify the load response to voltage variations as constant current load for the active power, and as constant impedance load for the reactive power. Considering the ST capability to reduce the voltage up to 10%, the amount of power reduced for a residential grid can be estimated in 10% active power and up to 20% of reactive power. Considering a power factor of 0.9 pu, the total apparent power that can be controlled results be 20%.

The power generation in the LV grid is independent from the voltage amplitude. The voltage control performed by the ST cannot modify the generators power injection, being not sensitive to voltage variations. However, controlling the frequency, the ST can interact with the droop controller of the distributed generators in LV grid and modify their power injection [10, 12]. While a power reduction is technically feasible [10], increasing the power of the generators depends on the availability of controlled resources in the LV grid. The renewables do not have usually reserve energy to be employed in this case, and thus appliances like microturbines, diesel generators or storage systems are needed for providing upwards regulation capability to the ST. The current LV grid takes the direction of implementing more controllable generation and load in the "Smart Grid" vision [20]. Although in few years the grid will be fully controllable, it can be assumed that the controllable generation installed in LV grid can cover up to 10% of the load consumption.

Considering the ST features, a total apparent power controllability of 20% is estimated. Thus, the ST size can be decreased by 20% with respect to the conventional transformer design. In this context, an innovative ST design approach named “Grid-Tailored-Design-Approach” (GTDA) is proposed. Applying the GTDA, the power converters of the ST are used in more efficient way, resulting in cost and footprint reduction. On one hand, if more grid services are desired, a power converter stage may presents higher cost, depending on the service. On the other hand, the saving in one or more stages can be used to compensate for the extra cost of the other stage (due to the additional service), keeping the total cost comparable to the one from the convention design. The GTDA has the advantage of providing more services at the same cost of the SST or conventional transformer design.

As an example, the MV converter can be sized following two strategies: the minimum cost or the inclusion of more grid ancillary services. The minimum cost strategy designs the MV side depending on the DC/DC converter size, minimizing the hardware expenses. The second strategy, instead, is based on sizing the MV converter in order to provide services to the MV grid, such as reactive power support. In this case, the cost saving from the LV side and DC/DC stages can be invested on the MV side stage, leading to a constant cost with the additional service of reactive power support. The Table IV shows the power level required for each ST stage, considering the different design approach. In this Table, the case A is the standard design approach, where each stage is designed for the same power, defined by the load. In case B, the load reduction service is applied in the LV, leading to a power reduction and consequently to the cost minimization. In that case, all stages are designed for the same power level. In case C, the GTDA is considered, and the cost saved in the LV and DC/DC stages is invested in the MV side, to provide more reactive power to support the MV grid. These values are obtained based on the detailed design of the converters, including the calculation of the cost, as discussed in the next section.

Table IV. Definition of three-study cases

Design Cases		LV AC/DC (MVA)	DC/DC (MW)	MV (MVA)	Cost
Standard design	A	1.0	1.0	1.0	Standard
ST grid-tailored design (LV service)	B	0.8	0.8	0.8	Minimum
ST grid-tailored design (LV service + MV services)	C	0.8	0.8	2	Standard

V. GTDA design procedure

In order to design a ST using the GTDA, the topology shown in Fig. 3 (a), as well as the specification presented in Table I, are used. The ST is designed considering the three cases presented in Table IV.

For each converter, the sizing is based on the semiconductor selection, cooling system and capacitor bank. These components are designed following the equations (1) to (4).

A. Design Considerations

• Semiconductors Design

The semiconductors are selected considering the maximum blocking voltage and the average current flowing through them. For each case shown in Table IV, the power processed by the converter is affected, but the voltage levels are constant. The selection is made on the average current and the power dissipated in each device (1). For the power semiconductors selection, the available IGBT power modules from *Infineon Technology* (with Dual configuration) is considered in the DC/DC and LV stages. For the MV stage, IGBT power modules from *Infineon Technology* and *Fuji Electric* are assumed. For price comparison purposes, the quotation is obtained from the same distributor (Mouser Electronics) and for the same amount of pieces (40 pieces).

• Cooling System Design

To design the cooling system of the power converter, the conventional approach based on the semiconductors power dissipation (P), ambient temperature (T_{amb}), junction temperature (T_j) and thermal resistance in the power path between the junction and the ambient (R_{th}) is considered [21]. To evaluate the influence of the services on the cooling system, the “cooling system performance index” (CSPI) approach [21] is used. Using this approach, a constant cooling profile is selected, leading to a constant CSPI, as defined in (3). The volume of the heatsink is proportional to the power dissipation, as described in (4). To compute the cost of the cooling system, it is assumed that the price of the heatsink is proportional to the volume. A constant CSPI is considered to keep the

junction temperature at 100°C for the device with lower losses, i.e. lower cooling system requirement. For the devices that dissipate more power, parallel heatsink blocks are considered.

- **Capacitor Bank Design**

The required capacitance is calculated according to the power processed by the converter [22], using (2) in Table III. As it can be seen, the required capacitance is directly related with the apparent power processed, for a given voltage ripple (ΔV_{MVDC}), and therefore it is directly influenced by the additional grid services. For the cost comparison, a basic capacitor block of 100 μF / 500 V is assumed, to be assembled in series/parallel according to the converter requirements.

The design solution for the LV side capacitor is based on setting the maximum voltage oscillation (i.e., 5%), employing equation (5). The capacitance is calculated taking in account the DC link nominal voltage and the possible current imbalance that can happen in the grid. This value can be obtained from historical data of the LV grid and knowing in advance of the presence of fixed three-phase loads (balanced by nature). If the peak-to-peak power oscillation is 300 kW and the system is working at nominal DC voltage of 700 V, a capacitance at least of 18mF is suggested.

Additionally, for the DC/DC stage, the transformer design is considered. For the three different cases, the same transformer core with different litz wires is assumed. Thus, for the cost comparison of the transformer, only the iron amount is considered. The cost of the magnetics is evaluated by employing textbook formulas [23]: from the effective current, the wire area and the number of turns is evaluated. As design parameters, switching frequency, peak flux and current density are considered constant, as well as the core size. From the copper volume, it is possible to calculate the estimated costs [24]. From these assumption, the volume of the copper is proportional to the processed power. Since the design is performed with the same DC voltage, the price of the copper is proportional to the effective current. For the cases B and C, less iron is used on the transformer, leading to the cost reduction. The wires are selected according to the effective current as presented in [15]. More detail on the design of this stage is presented in [15].

Table V . Grid and power converters specification

IGBT Losses	
$P = V_{CE} \cdot I_{ch(avg)} + r_{ch} \cdot I_{ch(rms)}^2 + V_f \cdot I_{d(avg)} + r_d \cdot I_d^2(rms)$	
<i>Channel losses</i>	<i>Body diode losses</i>
(1)	
MV side capacitor	
$C = \frac{S}{2 \cdot \pi \cdot f_{grid} \cdot \Delta V_{MVDC} \cdot V_{MVDC_{min}}^2}$	
(2)	
Cooling system	
$CSPI \left[\frac{W}{K \cdot dm^3} \right] = \frac{1}{R_{th}[K/W] \cdot V[dm^3]}$	
(3)	
$V = \frac{P \cdot \left(\frac{1}{\eta} - 1 \right)}{CSPI} (T_J - T_{amb})$	
(4)	
LV Side Capacitor	
$\Delta V_{pk-pk} = \frac{\Delta P_{pk-pk}}{2\pi f_H C_{LV}^{DC} V_{LV}^{DC}}$	
(5)	

A. Design Results Discussion

As a result of the design, the normalized required semiconductor, cooling system volume and capacitance for each design case are presented in Fig. 5, for each stage of the ST. In order to compare the influence of the semiconductors selection on the ST design, two semiconductors modules from different manufactures were assumed for the MV side, due to their high performance: FF150R17KE4 (1.7 kV/150A from *Infineon Technology*) and 2MBI75VA-170-50 (1.7 kV/75A from *Fuji Electric*). As can be noticed, the current rating of the Infineon Power Modules is twice the one from the Fuji Electric, implying in an underutilization of the first

one. Nevertheless, using the power module from Infineon, the current flowing through the channel is much smaller than the semiconductors current rating, leading to an operation point with small forward drop voltage ($V_{CE(on)}$). Consequently, the power dissipation is small, as well as the cooling system volume, as depicted in Fig. 5 (a). Note that the power semiconductor selection plays an important role in the ST design, affecting cost, efficiency and volume. Apart from its own cost, the semiconductor selection influences the cooling system cost and volume. Hence, the trade-off between these components must be considered. In this study, it is assumed a heatsink building block with a cost of U\$ 50. These blocks are parallelized if more cooling capability is required. For this particular case, an overall cost comparison of the MV stage considering those two different semiconductors is shown in Fig. 7. In spite of the high cooling system required by the *Fuji Electric* power modules (see. Fig. 5 (a)), the semiconductors price is considerably lower, compensating for the high investment in the cooling system. Therefore, the MV stage design using *Fuji Electric* is more viable economically.

Due to the higher power level in Case C, the semiconductor is better used than in case A and B. On the other hand, the amount of cooling system is much higher, since the power dissipation is also higher. For the LV side and DC/DC stages, the design for the cases B and C are the same, since the amount of processed power and voltage remains the same.

As already mentioned, in case C, the saving cost from the LV side and DC/DC is invested on the MV stage. Considering the results obtained and presented in Fig. 5, the saving cost is shared among the cooling system and capacitors, once the semiconductors of the MV remained the same. For this reason, a reduction of 20% of power in the LV and DC/DC stages allows to increase the power of the MVA of around 100% with respect to case A. Thus, for the assumed parameters, the MV stage can provide 2 MVA of apparent power, keeping the same overall system cost of case A. This is exemplified with the graphic of Fig. 6.

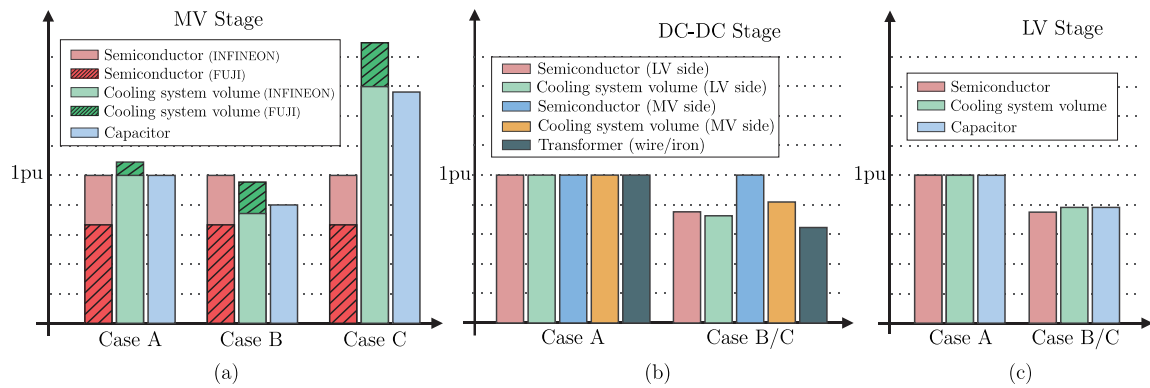


Fig 5. Design of the ST for the three different cases: (a) MV stage; (b) DC-DC stage and (c) LV stage.

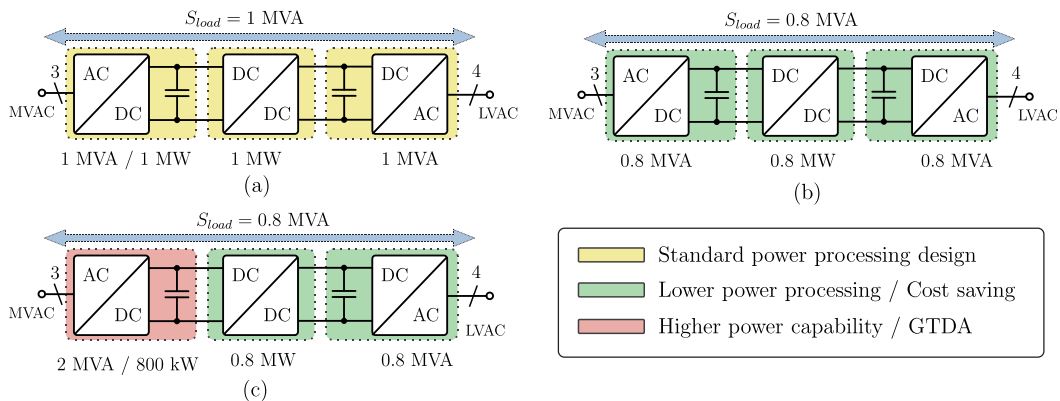


Fig. 6. The block diagram of the ST considering the three different design approaches, highlighting the power processed by each stage: (a) Case A: Standard design approach; (b) Case B: Standard Design, including the LV services to reduce the load consumption; (c) Case C: proposed Grid Tailored Design Approach (GTDA).

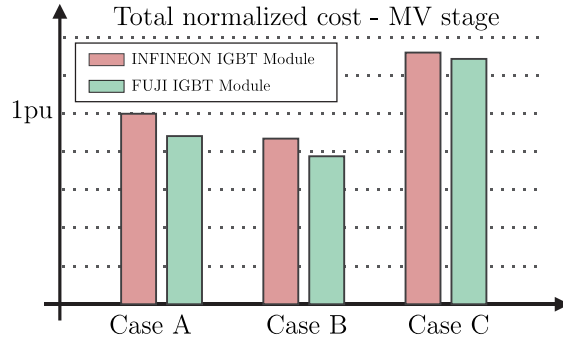


Fig 7. Cost comparison of the MV stage for different semiconductors power modules.

VI. Simulation case study of the proposed GTDA

Depending on the grid needs, the ST can provide different services: local voltage support, voltage control in a specific bus, and power factor control at the HV/MV substation busbar. The simplest service it can provide is the operation under unity power factor. The LV side converter produces the reactive power for the LV grid, and the MV converter can absorb only active power, reducing the reactive power burden of the MV grid. The ST injects reactive power to control the voltage at its busbar, or at a specific busbar in the grid. In a specific case, it can control the power factor at the HV/MV substation busbar, avoiding low power factor conditions (i.e., below 0.9 p.u.).

However, the reactive power injection depends on the MV converter size and the active power request in LV side (both AC and DC). The LV active power can be only partially regulated [6], but it affects the power quality in the grid. Instead, the size of the MV side converter can be tailored to the MV grid to have better control margins.

In Fig. 8 is shown a practical example of what described above. A load flow simulation has been performed on a modified IEEE 34-bus test feeder. The grid voltage adopted is 10 kV, in order to match with the ST considered in this work. The ST absorbs 700 kW of active power and the LV loads work with a power factor of 0.9 pu. The ST injects reactive power to its maximum capability to support the voltage profile. If the ST is sized following the conventional transformer or SST design strategy (Case A), the amount of reactive power injected is limited to 714 kVAR, not sufficient to keep the voltage at about 0.95 pu. For the Case B, the power processed by the ST is lower than the Case A applications. Thus, the amount of reactive power injected in MV grid is lower, and no voltage support can be given (green line in Fig. 8). With the proposed design approach in Case C, the ST can be undersized in the LV and DC/DC stages, and the MV converter can be increased up to 2 MVA, without increasing the transformer costs. However, the benefits for the MV grid are clear. With higher reactive power capability, the ST is able to sustain the voltage profile above 0.95 pu in the whole grid, guaranteeing a good quality of the service.

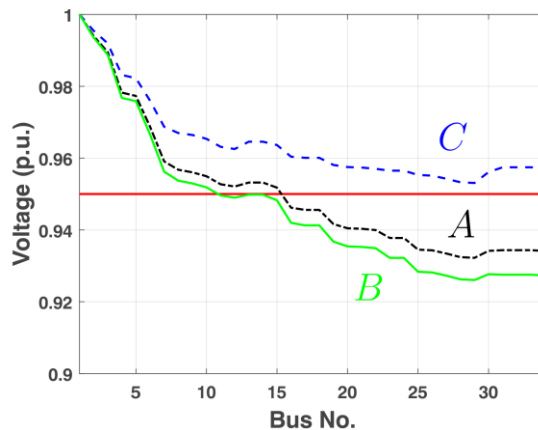


Fig. 8. Voltage profile in the modified IEEE-34 bus feeder in the design case A (point-dot black line), in the design Case B (continuous green line) and in the design case C (dotted blue line). The minimum voltage limits are marked (continuous red line, 0.95 pu).

VII. Experimental Results of the ST

In order to evaluate experimentally the operation of the ST, a downscaled prototype has been developed and tested. Table VI presents the specifications of the prototype, and Fig. 9 shows the prototype and the topology. In the MV side, the cells of the CHB and QAB are assembled together and share the cooling system. A peak efficiency of 94.5% was obtained with IGBT IHW40N120. To reduce the switching and conduction losses, SiC MOSFETs could be used, allowing for an increase of efficiency up to 97.5% (with C2M0025120D devices).

Table VI. Specification of the implemented prototype of the ST unit

Parameters	Value
Maximum Power	20 kW
Max AC voltage	1.4 kV RMS / 50Hz
Individual MVDC link	700 V
LVDC link	700 V
Isolation frequency	20 kHz

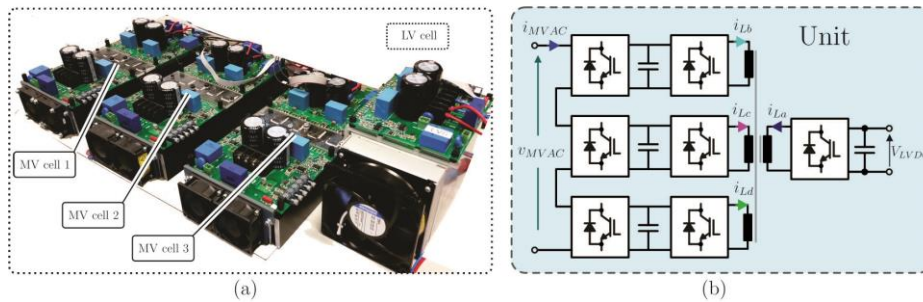


Fig. 9. Implemented a ST unit prototype based on the CHB and QAB converter and experimental results obtained from it: (a) picture of the prototype; (b) topology of the implemented power stage.

VIII. Conclusions and future research topics

In this paper, the design of a three-stage Smart Transformer is analyzed. The standard design flow for this system implies sizing each stage for the peak load request from the LV side. By exploiting the control functionality of the ST, however, a controllability margin exists to re-shape the load profile, effectively decreasing the power handling requirements from the LV and DC/DC stages. This feature is exploited by a Grid-Tailored-Design-Approach, where the cost saved in in the LV and DC/DC stage is re-invested in the MV stage, to make it able to process a greater amount of reactive power to guarantee MV voltage support. It is shown that the GTDA allows obtaining a ST design that can supply the same grid of an SST, but providing grid voltage support in the MV side at the same cost.

IX. Acknowledgment

The research leading to these results has received funding from the European Research Council under the European Union's Seventh Framework Programme (FP/2007-2013) / ERC Grant Agreement n. [616344] - HEART.

References

- [1]. A. Ipakchi and F. Albuyeh, "Grid of the future," in IEEE Power and Energy Magazine, vol. 7, no. 2, pp. 52-62, March-April 2009.
- [2]. E.J. Coster, J.M.A. Myrzik, B. Kruimer and W. L. Kling, "Integration Issues of Distributed Generation in Distribution Grids," Proceedings of the IEEE, Vol. 99, No. 1, Jan. 2011.
- [3]. P. P. Barker and R. W. De Mello, "Determining the impact of distributed generation on power systems. I. Radial distribution systems," 2000 Power Engineering Society Summer Meeting, Seattle, WA, 2000, pp. 1645-1656 vol. 3.
- [4]. M. Liserre, G. Buticchi, M. Andresen, G. De Carne, L. F. Costa and Z. X. Zou, "The Smart Transformer: Impact on the Electric Grid and Technology Challenges," in IEEE Industrial Electronics Magazine, vol. 10, no. 2, pp. 46-58, June 2016.
- [5]. X. She, A. Q. Huang, and R. Burgos, "Review of solid-state transformer technologies and their application in power distribution systems," IEEE Journal of Emerging and Selected Topics in Power Electronics, vol. 1, no. 3, pp. 186-198, Sept 2013.

- [6]. J. Wang, A. Q. Huang, W. Sung, Y. Liu, and B. J. Baliga, "Smart grid technologies," *IEEE Industrial Electronics Magazine*, vol. 3, no. 2, pp. 16–23, June 2009.
- [7]. J. W. Kolar, J. Huber, T. Guillod, D. Rothmund, F. Krismer, *Research Challenges and Future Perspectives of Solid-State Transformer Technology*, Keynote Presentations at the 5th International Conference on Power Engineering, Energy and Electrical Drives (POWERENG 2015), Riga, Latvia, May 11-13, 2015.
- [8]. G. De Carne; M. Liserre; C. Vournas, "On-line load sensitivity identification in LV distribution grids," in *IEEE Transactions on Power Systems*, Early Access.
- [9]. G. De Carne; G. Buticchi; M. Liserre; C. Vournas, "Load Control using Sensitivity Identification by means of Smart Transformer," in *IEEE Transactions on Smart Grid*, Early Access.
- [10]. G. De Carne; G. Buticchi; Z. X. Zou; M. Liserre, "Reverse power flow control in a ST-fed distribution grid," in *IEEE Transactions on Smart Grid*, Early Access.
- [11]. G. Buticchi, G. De Carne, D. Barater, Z. Zou, M. Liserre, "Analysis of the frequency-based control of a master/slave micro-grid", *IET Renewable Power Generation*, 2016, vol. 10, no. 10, p. 1570-1576.
- [12]. G. De Carne, G. Buticchi, M. Liserre and C. Vournas, "Frequency-Based Overload Control of Smart Transformers," 2015 IEEE Eindhoven PowerTech, Eindhoven, 2015, pp. 1-5.
- [13]. X. She, X. Yu, F. Wang, and A. Q. Huang, "Design and demonstration of a 3.6-kv 120-v/10-kva solid-state transformer for smart grid application," *IEEE Transactions on Power Electronics*, vol. 29, no. 8, pp. 3982–3996, Aug 2014.
- [14]. C. Zhao, D. Dujic, A. Mester, J. Steinke, M. Weiss, S. Lewdeni-Schmid, T. Chaudhuri, and P. Stefanutti, "Power electronic traction transformer;medium voltage prototype," *IEEE Transactions on Industrial Electronics*, vol. 61, no. 7, pp. 3257–3268, July 2014.
- [15]. L. Costa; G. Buticchi; M. Liserre, "Quad-Active-Bridge DC-DC Converter as Cross-Link for Medium Voltage Modular Inverters," in *IEEE Transactions on Industry Applications*, Early Access.
- [16]. J. D. Luze, "Distribution transformer size optimization by forecasting customer electricity load," 2009 IEEE Rural Electric Power Conference, Fort Collins, CO, 2009, pp. C2-C2-6.
- [17]. Z. Wang and J. Wang, "Review on implementation and assessment of conservation voltage reduction," *IEEE Transactions on Power Systems*, vol. 29, no. 3, pp. 1306–1315, May 2014.
- [18]. K. P. Schneider, J. Fuller, F. Tuffner, and R. Singh, "Evaluation of conservation voltage reduction (cvr) on a national level," Pacific Northwest National Laboratory report, 2010.
- [19]. J. V. Milanovic, K. Yamashita, S. Martínez Villanueva, S. Ž. Djokic and L. M. Korunović, "International Industry Practice on Power System Load Modeling," in *IEEE Transactions on Power Systems*, vol. 28, no. 3, pp. 3038-3046, Aug. 2013.
- [20]. H. Farhangi, "The path of the smart grid," in *IEEE Power and Energy Magazine*, vol. 8, no. 1, pp. 18-28, January-February 2010.
- [21]. U. Drofenik, G. Laimer, J. W. Kolar, "Theoretical Converter Power Density Limits for Forced Convection Cooling", *International PCIM Europe Conference (PCIM 2005)*, Nuremberg, Germany, pp. 608-619, June 7-9, 2005.
- [22]. Teodorescu, R.; Liserre, M.; Rodriguez, P. "Grid Converters for Photovoltaic and Wind Power Systems", WILEY, 2011.
- [23]. M. K. Kazimierczuk, *High-Frequency Magnetic Components*. Wiley Publishing, 2009.
- [24]. <http://www.nasdaq.com/markets/copper.aspx>, accessed in 04.02.2017.

X. Appendix A

The IGBT power module available on the market from the main semiconductors are summarized in Table VII. Notice that only Dual configuration is assumed in this table. Table VIII presents the considered IGBT power module for cost analysis carried out in this paper. These power modules are from *Powerex* manufacture, also with Dual configuration. The cost was obtained directly with the manufacture on 20.02.2017.

Table VII. Available IGBT on the market considering the main manufactures.

Voltage Rating (V)	Manufacture	Current (A)	Configuration	Partnumber
6500	Powerex	85	Dual	QIC6508001
	Mitsubishi	750	Single	CM750HG-130R
	Infineon	250	Single	FZ250R65KE3
3300	Powerex	100	Dual	QID3310006
	Mitsubishi	1000	Single	CM1000HC-66R
	Infineon	200	Dual	FF200R33KF2C
	Fuji	800	Single	1MBI800UG-330
1700	Powerex	75	Dual	CM75DY-34A
	Mitsubishi	75	Dual	CM75DY-34A
	Infineon	150	Dual	FF150R17KE4
	Fuji	75	Dual	2MBI75VA-170-50
1200	Powerex	50	Dual	CM50DU-24F
	Powerex	75	Dual	CM75DU-24F
	Mitsubishi	100	Dual	CM100DY-24NF
	Infineon	50	Dual	FF50R12RT4
	Infineon	75	Dual	FF75R12RT4
	Fuji	75	Dual	2MBI75VA-120-50

Table VIII. Considered IGBT power module for cost analysis from *Powerex* manufacture and Dual configuration.

MV side				LV side			
Voltage Rating (V)	Current Rating (A)	Reference	Cost (US\$)	Voltage Rating (V)	Current Rating (A)	Reference	Cost (US\$)
1200	300	CM300DX-24S1	137,39	6500	150	QIC6508001	689
	200	CM200DX-24S	145,01	3300	100	QID3310006	539
	150	CM150DX-24S	110,37	1700	75	CM75DY-34A	120
	100	CM100DY-24A	99,65	1200	50	CM50DU-24F	80,31
	75	CM75DU-24F	98,55				
	50	CM50DU-24F	80,31				

XI. Appendix B

The detailed values obtained from the QAB design and DAB design, used in the comparative analysis of these converter are presented in Table IX.

Table IX. Detailed values obtained from QAB and DAB converters design.

Parameters	QAB		DAB	
	LV side	MV side	LV side	MV side
Number of units	9 (3 per phase)		27 (9 per phase)	
Unit power level	111.11 kW		37.04 kW	
DC link voltage	700V	1.13 kV	700V	1.13 kV
Semiconductor voltage rating	1.2 kV	1.7 kV	1.2 kV	1.7 kV
Semiconductor mean current	84 A	17.6 A	28 A	17.6 A
Current rating	150 A	75 A	50 A	75 A
Selected semiconductor	CM150DX-24S	CM75DY-34A	CM50DU-24F	CM75DY-34A
Device cost	US\$ 110,37	US\$ 120,00	US\$ 80,31	US\$ 120,00
Basic cell cost	US\$ 1986,66	US\$ 6480,00	US\$ 4336,74	US\$ 6480,00
MFT rms current	184 A	38 A	61 A	38 A
Required inductance (LV side)	17.3 uH		51.8 uH	